

# Design and Drop Test of Sounding Rocket Parachute System

Nicholas M. Gaug<sup>\*</sup>, Harry A. Shrager<sup>†</sup>, Michael Peña<sup>‡</sup>, Vincent Nguyen<sup>§</sup>, Morgan Gregg<sup>¶</sup>, Alfonso Lagares de Toledo<sup>||</sup>  
*Georgia Institute of Technology, Atlanta, GA, 30332*

**The Georgia Tech Experimental Rocketry team designs, builds, and launches two stage high altitude sounding rockets. In order to accommodate the environments at higher altitudes and implement weight savings, a novel parachute system architecture has been developed for recovering the second stage of these vehicles. In order to validate the functionality of this parachute system in advance of its first flight on Georgia Tech's Material Girl sounding rocket, two tests were performed in which it was dropped from an aircraft and deployed in freefall. These tests aimed to simulate the dynamic and aerodynamic environment experienced by the recovery system during deployment at apogee. A test article was developed representing the upper section of the second stage of Material Girl, including internal parachute hardware. An electronic arming system allowing a human operator aboard the aircraft to safely and effectively activate and release the test article was developed and is described. During the first drop test, issues with the parachute system leading to an unsuccessful deployment were identified. Changes were made to the system to address these issues and are discussed. The second drop test achieved a successful deployment. The performance of the parachute system during both tests is also analyzed and discussed.**

## I. Introduction

THE successful deployment of parachutes is paramount to the success of a sounding rocket flight in which any portion of the rocket or payload must be recovered. For a successful parachute deployment, the associated recovery system must achieve proper timing, separation of the parachute from the inner structure of the rocket, and uninhibited unraveling and inflation of the parachutes. In amateur and collegiate rocketry, shortcomings in one of these areas often lead to unsuccessful deployments and subsequent loss of the vehicle. The difficulties associated with proper deployment rise dramatically as both the size of a rocket and the height of its apogee increase. In order to mitigate the challenges associated with high altitude parachute deployment, the Ramblin' Rocket Club (RRC) has developed a novel parachute system for flights on future sounding rockets, beginning with the *Material Girl* sounding rocket launched in 2023 [1]. This system provides a significant reduction in complexity when compared with the recovery systems employed on rockets of similar size and scope. It also occupies a significantly smaller internal volume, which leads to increased performance due to size and weight savings.

Collegiate rocket teams often use two parachutes for descent - a drogue parachute, to stabilize descent at high speed (about 15-20 m/s) in the upper atmosphere, and a main parachute, to slow down for a soft landing (about 6 m/s) in the lower atmosphere. However, RRC instead employs an "all-drogue" parachute architecture. This means that each rocket stage descends under a medium sized drogue parachute, which is deployed at apogee, without a main parachute. This reduces rocket dry mass, minimizes drift while under parachute descent (even from high altitudes), and greatly reduces the required complexity of the recovery system and onboard electronics. The main drawback is a greatly increased ground impact velocity, which poses the risk of damaging lower-mounted components, such as the motor nozzle and fins. However, the expected impact velocity, while higher than what would be seen under a traditional parachute architecture, is agreed upon to remain low enough to mitigate damage to important hardware.

RRC's current parachute architecture was conceived as a result of two significant parachute failures. During the flight of *Rubber Band Man* in 2021, the main parachute of the second stage failed to deploy. This was because the small device designed to retain the main parachute within the airframe (or body tube of the rocket) during the period of descent under the drogue parachute did not properly activate. During the flight of *Mr. Blue Sky* in 2022, which had made the

<sup>\*</sup>Undergraduate Student, School of Aerospace Engineering, ngaug3@gatech.edu, AIAA Student Member 1229066

<sup>†</sup>Undergraduate Student, School of Aerospace Engineering, hshrager3@gatech.edu, AIAA Student Member 1603506

<sup>‡</sup>Undergraduate Student, School of Aerospace Engineering, mpena38@gatech.edu, AIAA Student Member 1342439

<sup>§</sup>Undergraduate Student, School of Mechanical Engineering, vnguyen343@gatech.edu, AIAA Student Member 1603503

<sup>¶</sup>Undergraduate Student, School of Aerospace Engineering, mgregg31@gatech.edu, AIAA Student Member 1400677

<sup>||</sup>Undergraduate Student, School of Aerospace Engineering, alagares@gatech.edu, AIAA Student Member 1314883

switch to the all-drogue architecture, the drogue parachute of the 2nd stage failed to leave the airframe after the nosecone separated. The new parachute architecture described in this paper is designed specifically to mitigate these issues. RRC sought to verify the functionality of this new architecture in a representative flight environment before implementing it on future sounding rockets. To this end, a test article was built which represents the upper stage of a sounding rocket and contains all the relevant internal components comprising the recovery system. This article was dropped twice from an aircraft and deployed midair. The flight test was designed to represent as closely as possible the flight conditions seen by a rocket at apogee during parachute deployment. By verifying the functionality of this parachute system through these drop tests, the successful deployment of parachutes can be ensured on future RRC sounding rocket flights.

## II. System Design

### A. Parachute System Design

The parachute system described is designed for deployment from the top of a 15 cm diameter airframe tube, capped off by a nosecone. This system consists of two parachutes, one attached to the rocket/airframe, and one attached to the nosecone, which is separated from the top of the airframe upon deployment. The airframe parachute is a 1.5 m diameter reinforced parabolic parachute (drag coefficient of 0.97), connected (through a 13.3 kN-rated swivel) to the internal structure of the airframe by two lengths of 9 m long, 14 kN-rated nylon shock cord. The nose cone parachute is a 0.6 m diameter lightweight parabolic parachute, connected to the nose cone by another 9 m long, 14 kN-rated shock cord. Because the pyrotechnic charges are located in the airframe tube, pointing upwards into the parachute bay, the first 5 feet of the airframe parachute's shock cords are sleeved in Nomex fabric, and the parachute itself is wrapped in a Nomex deployment bag (connected using paracord), which has an integrated pilot parachute to pull itself off during deployment. The deployment bag serves as both heat protection and also slows down parachute inflation to reduce overall forces of deployment. The pre-deployment shock cords are stored above the deployment bag while inside the nose cone, to shield them from the pyrotechnics. The initial design of the parachute rigging was verified using data and calculations from [2] and [3].

Two extra methods to slow down parachute inflation were also implemented. All shock cords and shroud lines are z-folded separately and bound in rubber bands to prevent them from unraveling and inflating too rapidly. In addition, a reefing ring was installed at the top of the airframe parachute's shroud lines to slow down parachute inflation.

Finally, two auxiliary tracking methods were also added, which were implemented as backup recovery methods. These consist of a Radio Direction Finding (RDF) system and strobe lights attached to the shock cords on each parachute. The RDF system is implemented as a set of small radio beacons, one per individual parachute, placed in small pouches and directly mounted to each parachute at the bottom of the shroud lines. See Section II.C for more information. The strobe lights are implemented as off-the-shelf emergency beacons, mounted halfway up one of the shock cords in each parachute system using adhesive tape. These were intended to be a last-resort recovery method, the concept being to locate the components visually after nightfall by searching for the bright flashes created by the strobe lights. Fig. 1 shows a schematic of the parachute rigging as described.

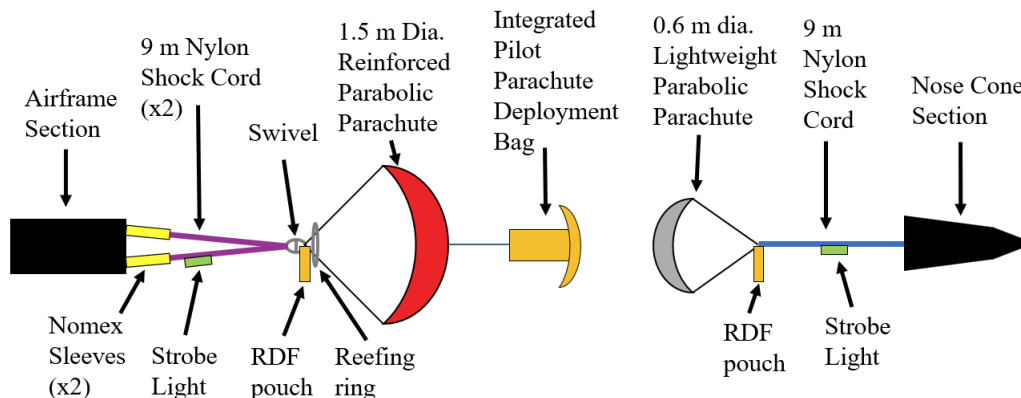


Fig. 1 Schematic of 2nd stage parachute rigging, not to scale, as tested on the first drop test.

## B. Drop Test Article Design

The drop test article is a representative nose cone and truncated section of the fin can, containing the necessary subsystems to simulate the deployment of parachutes during vehicle flight. The article's exterior is made of a carbon fiber tube 15.24 cm in internal diameter and 36 cm in length, and a truncated fiberglass nose cone 77.47 cm in length. The size of the article was chosen to match the volume of the full-scale deployment system, with additional internal space for drop test-specific avionics.

The nose tip was machined from stainless steel and is attached to the nose cone via a conical nut that is epoxied to the inside edge of the truncated nose cone. The nose tip had a tapped hole in which a threaded rod containing a small avionics bay was attached. The avionics bay contained a GPS tracker and a 400 mAh lithium polymer battery. A custom eye nut was threaded to the end of the rod and served as the anchor point for the nose cone parachute. Between the nose cone and the fin can, a fiberglass coupler 15.24 cm in external diameter and 20.32 cm in length was used to add bending rigidity and serve as the connection point between the nose cone and the fin can.

Below the coupler, the fin can contained a 15.24 cm diameter aluminum ring, called the parachute ring. The parachute ring was anchored to the carbon fiber air frame with twelve radial bolts. The cords from the fin can parachute were attached to the parachute ring with two stainless steel dowel pins set within the ring. Below the parachute ring, a G10 plate of 0.3175 cm thickness was secured to the ring with three radial bolts and an epoxy fillet. The fillet also served as a pressure seal between the charge well bay and the avionics. The G10 plate was referred to as the charge well plate, and held two 1.54 cm diameter pyrotechnic charge wells on the top side and the article's avionics on the bottom side. Two charge wells were used for redundancy, and were electrically connected to the avionics on the opposing side of the charge well plate with an epoxy-sealed pass through. The bottom of the article was capped with an aluminum plate of .3175 cm thickness meant to shield the avionics from the environment and contained a cutout for the button, with enough room for the operator to grip the article. A schematic of the vehicle is shown in Fig. 2.

The number of radial bolts, the diameter of dowel pins, and the thickness of the charge well plate were calculated to withstand the expected forces of shear from the parachute and force of pressurized gas from the pyrotechnic charges during deployment. The chemical used in the charges was Boron Potassium Nitrate (BPN), which is described in detail in [4]. Prior to ground deployment testing, each structural component was experimentally tested to determine each failure point, and the factor of safety of each component was scaled to make the shock cord attachment at the pins the weakest point. Through experimentation, the factor of safety was determined to be 1.28 with the main failure point originating at the rods securing the shock cord to the article.

Prior to the drop test, the full article was validated through two ground deployment tests, where the mass of BPN required to shear the rivets attaching the nose cone to the air frame was experimentally determined. Through ground deployment testing, the team validated the integration method of the article and the successful shear of the shear rivets in the nose cone. Ground deployment testing revealed the greatest loss in pressure within the charge well bay to be a result of improper sealing between the charge well bay and the avionics bay, and buckling of the G10 charge well plate. Ground deployment testing drove design changes to add a rubber gasket between the parachute ring and the charge well plate and increase the thickness of the charge well plate from 0.3175 cm to 0.47625 cm. These changes yielded successful parachute deployment and sealing of the charge well bay, giving the team high confidence in the system prior to the drop test.

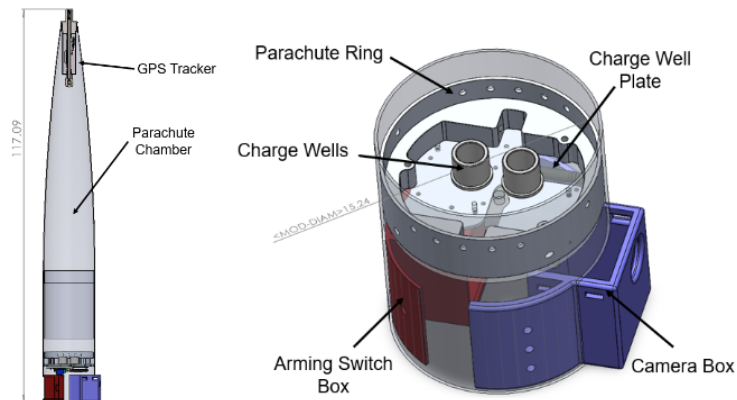


Fig. 2 Schematic of full drop test vehicle (left) and bay assembly (right)

### C. Avionics System Design

The parachutes on the rocket for which this parachute system was designed were intended to be deployed by a complex avionics suite capable of detecting apogee and executing other flight events. To imitate these avionics in the flight test article, a system was developed which was capable of three primary functions: arming, pyrotechnic charge activation, and GPS tracking. A combination of reliable commercial off the shelf (COTS) components were selected for these purposes to mitigate potential manufacturing errors and decrease the complexity of the system. An Arduino Nano served as the microcontroller to fire the pyrotechnic charges and interface with the arming system. This microcontroller was chosen based on its compact size, board mounting abilities, and wide range of applications. A relay was connected to a pin on the microcontroller which allowed enough current to pass through the e-match and cause ignition of the pyrotechnic charges. This ignition system had the ability to fire two redundant pyrotechnic charges thanks to its dual relay design. Six additional pins were utilized for the firing controls and safety features. The firing controls were composed of an arming switch and button, while the safety features included a RGB LED and buzzer. A standalone Featherweight Altimeters GPS Tracking system was onboard and was used for locating the article after upon landing. Two radio trackers were added as additional tracking on the test article. Both were located along the shock cords of the parachutes within flame resistant sheaths. A block diagram of the main avionics components used for controlling deployment is shown in Fig. 3.

During the design of the avionic system and associated arming logic, the safety of the human operator was the top priority. In order to create a robust and safe system, the following arming logic was implemented: to initiate the deployment sequence, the operator would toggle the arming switch, activating the arming button. The operator would then depress the arming button, and prepare for release. Once the arming button was released, a four second timer would begin, at the end of which the pyrotechnic charges would be activated. This way, the countdown to activation does not start until the test article has completely cleared the aircraft. At each step of this process, the LED and buzzer are programmed to indicate which phase of the sequence the system is in. The system could be disarmed at any point in the sequence by toggling the arming switch off. The arming logic is illustrated in Fig. 4.

The avionics within the test article also served to document the deployment of the recovery systems. A simple camera system composed of RunCams and GoPro 360 were used for this purpose. A RunCam was mounted on the forward end of the charginwell plate and a GoPro 360 was mounted to the airframe facing outward to capture parachute deployment.

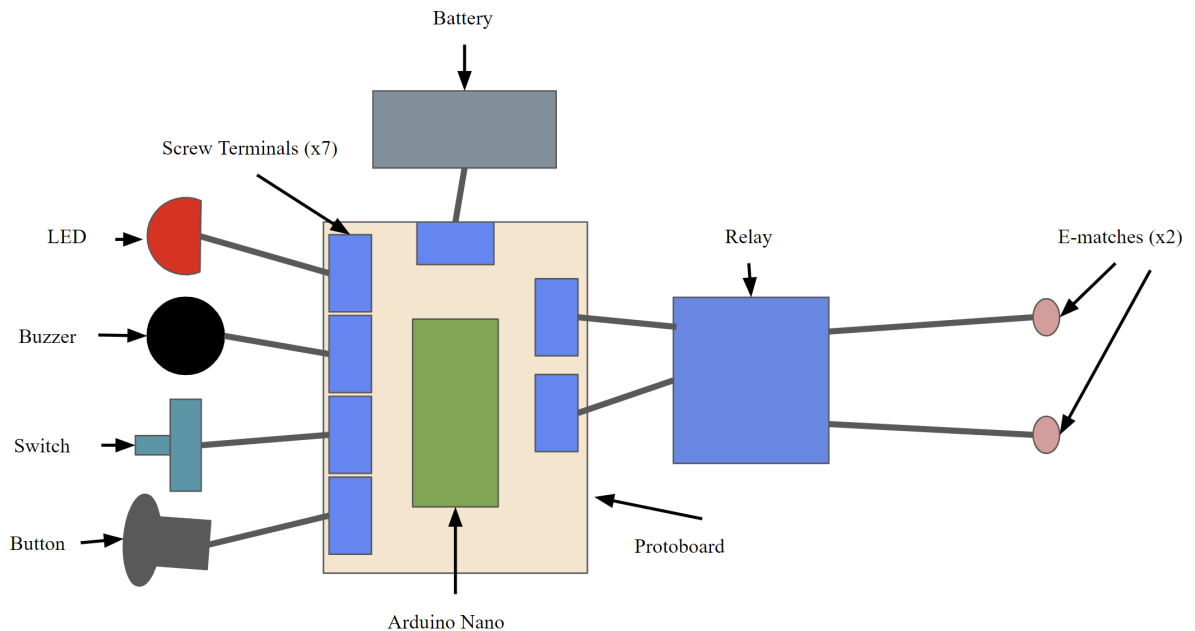


**Fig. 3 Schematic of avionics arming and safety hardware, not to scale, used in both drop tests**

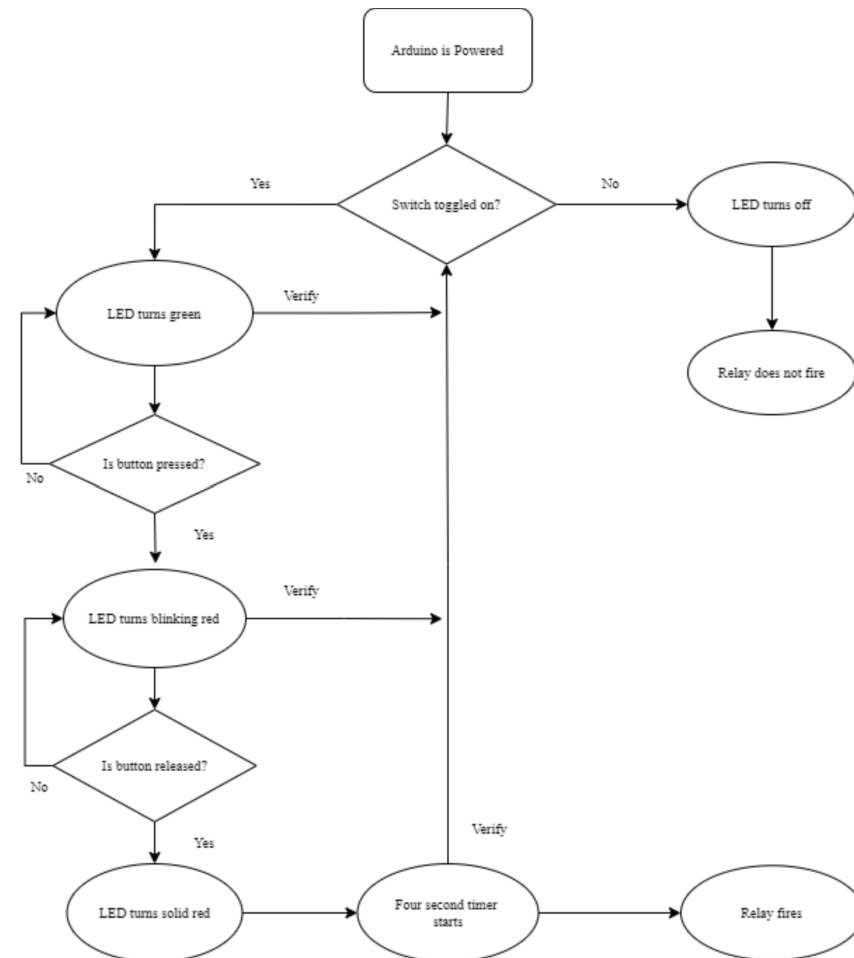


**Fig. 4** Flow chart depicting the arming and firing sequence for Drop Test pyrotechnics

### III. Test Design

In the testing of parachute systems, the most important parameter to hold constant between flight and testing is the dynamic pressure  $q$  at the moment of parachute deployment [5]. The present recovery system is designed to deploy at apogee. At the apogee altitude of the rocket for which the recovery system was designed, the atmospheric density is extremely low. However, flight simulations showed that there is a potential for a large component of horizontal velocity at apogee due to wind and non-zero launch angles. Therefore, the dynamic pressure could be nearly matched by a plane flying relatively slowly but at a lower altitude with a higher density. Based on flight simulations, a targeted speed of 100 m/s and altitude of 460 m were selected initially. The dynamic pressure achieved under these conditions is slightly lower than what is seen at apogee. However, the altitude is constrained by the need to have ample freefall time for deployment, and the speed is constrained by the maximum cruise performance of the aircraft utilized. The altitude was later increased to 1500 m to allow more freefall time during the second drop test. The drop test were conducted from a Cessna 208 aircraft outfitted for skydiving. The test article was armed and hand launched out of the open side door of the aircraft. After a programmed two second delay from the release of the deadman switch, the pyrotechnic charges were fired by the onboard computer and the parachutes were deployed. Caution was taken to ensure that the article would not impact people or property on the ground. Radio trackers and GPS units were attached to aid in locating the article after landing. Onboard and ground based cameras were used to capture the deployment sequence for analysis. The integrated drop test vehicle is shown being released from the Cessna 208 aircraft in Fig. 5.



**Fig. 5** Drop test article being released from Cessna 208 aircraft at 460 m AGL during first drop test

## **IV. Results and Discussion**

### **A. Results and Analysis of First Drop Test**

The first drop test saw the article released from the aircraft at an altitude of approximately 450 m. The article separated exactly as intended, and at the correct time. However, two major issues were observed during descent: the nose cone parachute failed to deploy and the airframe parachute canopy failed to inflate. As a result, the nose cone entered free fall, while the airframe descended at a higher than expected velocity. Fig. 6 shows the two components descending as described. The airframe parachute's failure to inflate was traced to having overall too much friction in the system which slowed down the inflation. The sources of this friction were the sets of rubber bands, the reefing ring, and the tight-fitting deployment bag. The combined effect of these systems was over-restricting the inflation of the parachute. The nose cone parachute's failure to leave the nosecone was traced to lack of airflow or any other force pulling the parachute out of the nosecone. A minor issue observed was the nomex sleeves on the airframe shock cords seeming to move up along the cords. This caused them to expose some of the nylon cordage to BPN soot (which spread through the parachute bay during separation), damaging the cords.



**Fig. 6** The drop test airframe (top left) and nosecone (bottom) falling away from the airplane during the first drop test.

## B. Modifications After First Test

After identifying the issues mentioned above during the first drop test, several changes were made to the parachute rigging to mitigate these issues. To prevent constraining the airframe parachute and preventing inflation, the rubber band bindings and the reefing ring were fully removed. The deployment bag was also removed and replaced with a 0.9 m square Nomex parachute protector, wrapped around the parachute and shock cords in such a manner as to unravel during deployment. This allows for the shock cords to pull apart the parachute protector as they unravel, exposing the airframe parachute to the airflow. However, the parachute protector, instead of being attached to the airframe parachute, was attached to the top of the nose cone parachute, causing both parachutes to pull on each other as the rigid airframe and nose cone travel apart. This assists with extracting both parachutes from the airframe and nose cone, while still allowing them to separate once the parachute protector unravels. Fig. 7 shows a schematic of the revised rigging when fully deployed.

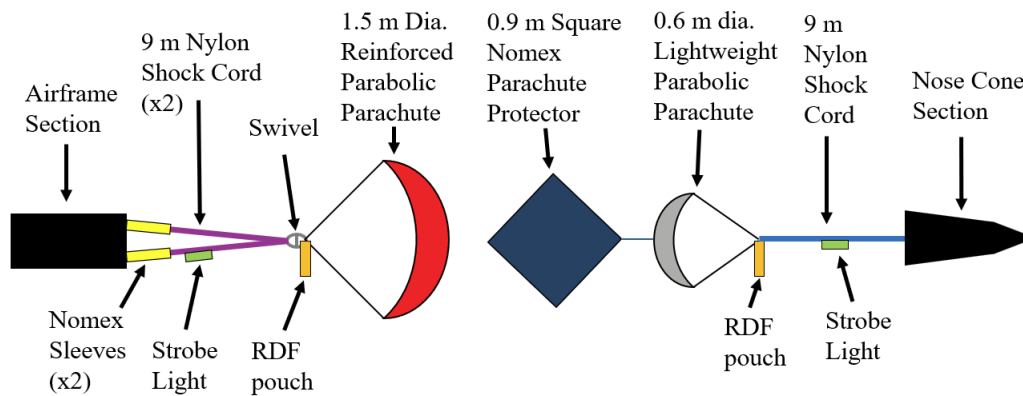


**Fig. 7 Schematic of 2nd stage parachute rigging, not to scale, as tested on the second drop test.**

To prevent the Nomex shock cord sleeves from moving along the airframe shock cords, they were affixed in position for this test using adhesive tape at the base of those cords.

## C. Results and Analysis of Second Drop Test

The second drop test saw the article released from the aircraft at an increased altitude of approximately 1500 m, to give more time before impact and to better observe the parachutes under descent. The article, once again, separated exactly as intended and with the proper timing after being dropped. As intended, both parachutes deployed, with the nose cone parachute inflating first, followed by the sustainer parachute. Fig. 8 shows the nose cone (bottom) and airframe (top) falling separately after deployment, with parachutes still unraveling in between the bodies.

One new issue was noted from the test: the airframe parachute's shock cord trapped itself inside the airframe parachute protector, as seen in the third image of Fig. 9. This resulted in the airframe parachute not deploying on time, causing the airframe itself to pull down on the parachute protector, hitting the inflated nose cone parachute canopy and causing that parachute to permanently collapse on itself and tangle. As a result, the nose cone parachute, despite initially deploying and inflating properly, still ended up descending at greatly increased speed. However, the airframe parachute canopy still inflated as expected and descended smoothly the entire way down.

The cause of the stuck shock cord was traced to the strobe light affixed to the airframe parachute's shock cord. The strobe light's bulky profile trapped it inside the folds of the still-unraveling parachute protector, preventing the airframe parachute from deploying, and thus inflating, on time. The adhesive tape on the airframe shock cord's Nomex sleeves, intended to hold it in position, was observed after recovery to have charred and failed during the initial separation. This resulted in the sleeves moving upwards again, resulting in the lower 15 cm of the the nylon shock cords becoming exposed to BPN soot again and sustaining damage.

To mitigate further issues, it was decided to remove the airframe parachute's strobe light and reduce the size of the parachute protector to a 0.75 m square in order to prevent the airframe shock cords from tangling again. The light in particular was fully removed because the drawbacks of it potentially disrupting parachute deployment were deemed to outweigh the benefits of having a third tracking method. In addition, to minimize the timeframe for the parachute rigging

to fully extend, the nose cone parachute's shock cord was shortened from 9 m to 3 m. This also had the advantage of reducing the occupied volume in the nose cone, allowing for looser packing and thus faster deployment.

The Nomex sleeves were prevented from moving up the shock cords by stitching 5mm holes in each sleeve, sized for the shock cord dowel pins to also pass through them, too. This constrained the Nomex sleeves in place and prevented them from further motion.



**Fig. 8** Nosecone (lower) and airframe (upper) falling away from airplane after deployment during the second drop test.



**Fig. 9** Sequence showing test article deployment. The first image shows the test article under freefall pre-separation. The second image shows the article moments after separation, with the airframe parachute protector visible. The last image shows the nose cone parachute and parachute protector.



## V. Conclusion

Two drop tests were conducted, and underlying issues with the recovery system architecture were effectively identified. Through modifications between the first and second tests, success was achieved in deploying the airframe parachute, which represents the most valuable part of a sounding rocket to be recovered. The test provided partial validation of the recovery system in advance of future sounding rocket flights, and identified future areas of improvement. The drop testing method described is validated as an effective means of assessing the performance of sounding rocket recovery systems.

## Acknowledgements

The authors would like to thank Jack Broadhead (Georgia Institute of Technology) for his advice and experience in parachute rigging and skydiving. They also thank Skydive Spaceland Atlanta for allowing the use of their site and aircraft for testing. The Authors would like to sincerely thank the the Georgia Tech Student Government Association, Georgia Tech Aerospace Engineering Department, and all club sponsors for the financial contributions that have made this work possible.

## References

- [1] Garud, P., Johnson, C., and Lagares de Toledo, A., "Material Girl Launch Report," Tech. rep., Ramblin Rocket Club, 2024. URL [rocketry.gatech.edu](http://rocketry.gatech.edu).
- [2] Knacke, T. W., *Parachute Recovery Systems: Design Manual*, Para Publising, 1992.
- [3] Newland, R., *Parachute Recovery System Design For Large Rocket Vehicles*, Aspire Space, 2020.
- [4] Peña, M., Tennant, V., and Gregg, M., "The Use of Boron Potassium Nitrate (BKNO<sub>3</sub>) in Recovery Deployment Systems for Hight Altitude Sounding Rockets," *AIAA Region II Student Conference*, 2024.
- [5] Jodehl, J., Anton, S., Bosboom, T., Dhiyaneeswaran, S., Dvorak, O., Homola, M., Knöll, N., Menting, E., Sujahudeen, M., Pepermans, L., et al., "Architectures for parachute testing," *72nd International Astronautical Congress*, 2021.